Journal of Medicinal Chemistry Article

*J. Med. Chem.* **2010,** *53,* 4877–4890 **4877**
DOI: 10.1021/jm901876r

# Exofacial Protein Thiols as a Route for the Internalization of Gd(III)-Based Complexes for Magnetic Resonance Imaging Cell Labeling

Giuseppe Digilio,[†] Valeria Menchise,[‡] Eliana Gianolio,[§] Valeria Catanzaro,[§] Carla Carrera,[§] Roberta Napolitano,[§] Franco Fedeli,[§] and Silvio Aime*[,§]

[†]*Department of Environmental and Life Sciences, University of Eastern Piedmont "A. Avogadro", Viale T. Michel 11, I-15121 Alessandria, Italy,* [‡]*Institute for Biostructures and Bioimages (CNR), c/o Molecular Biotechnology Center, University of Turin, Via Nizza 52, I-10125 Torino, Italy, and* [§]*Department of Chemisty, IFM and Center for Molecular Imaging, University of Turin, Via Nizza 52, I-10125 Torino, Italy*

*Received December 20, 2009*

Four novel MRI Gd(III)-based probes have been synthesized and evaluated for their labeling properties on cultured cell lines K562, C6, and B16. The labeling strategy relies upon the fact that cells display a large number of reactive exofacial protein thiols (EPTs) that can be exploited as anchorage points for suitably activated MRI probes. The probes are composed of a Gd(III) chelate (based on either DO3A or DTPA) connected through a flexible linker to the 2-pyridyldithio chemical function for binding to EPTs. GdDO3A-based chelates could efficiently label cells (up to a level of $1.2 \times 10^{10}$ Gd(III) atoms/cell), whereas GdDTPA-based chelates showed poor or no cell labeling ability at all. Among the GdDO3A based compounds, that having the longest spacer (compound GdL1A) showed the best labeling efficacy. The mechanism of EPT mediated cell labeling by GdL1A involves probe internalization without sequestration of the Gd(III) chelate within subcellular structures such as endosomes.

## Introduction

The concept of tissue repair through transplantation or grafting of suitable progenitor/stem cells is gaining more and more strength as the forthcoming therapeutic answer to several currently untreatable diseases. Cells can be "instructed" to repair damaged tissues, and cells can find their way to the tissue that has to be repaired. The development of cell-based therapies will greatly benefit from any method allowing for a noninvasive and repetitive monitoring of the delivery of repairing cells to the microenvironment of interest. The possibility of visualizing cell differentiation or response to biochemical stimuli would also be of immense value. "Cellular imaging" is a relatively new and very rapidly evolving branch of in vivo imaging techniques devoted to provide answers to these needs.[1−4] Among the armory of available in vivo imaging techniques, MRI[a] is one of the most promising because of its great spatial resolution (< 100 $\mu$m with modern high field equipment), lack of invasiveness (no ionizing radiation), and ease of adaptability to the clinical practice. Cells to be visualized by MRI must be labeled with suitable compounds, often referred to as "contrast agents" or "imaging probes". Because MRI suffers from low inherent sensitivity, cells to be tracked must be heavily labeled with suitable paramagnetic contrast agents (CA) for MRI detection to be possible. This makes it mandatory to develop highly sensitive MRI labeling agents and/or to optimize strategies to accumulate a large number of these agents to cells for visualization.[5] Labeling procedures typically involve the internalization of the imaging reporters. For instance, a very high MRI sensitivity has been obtained by loading cells with nanosized superparamagnetic iron oxide (IO) particles as $T_2$-contrast agents (these agents produce dark-spot image contrast, being henceforth also called negative agents).[6,7] Efficient loading (up to $(0.5-2) \times 10^7$ nanoparticles per cell) with IO particles was achieved by coating the particles with dextran to improve biocompatibility and by further functionalization of the dextrane surface with a HIV-tat derived peptide sequence as the membrane penetrating vector.[8] If positive image contrast is sought (bright spot image contrast), Gd(III) complexes are best suited.[5,9−11] The most direct route for the internalization of Gd(III)-based CAs takes advantage of pinocytosis, a physiological cellular process characterized by the spontaneous invagination of the cell membrane to form endosomal vesicles. During this process, CAs added at high concentration in the culture medium (50−100 mM) can be internalized to a significant extent. By this procedure it has been possible to load several kinds of cells, including stem cells, with suitable levels of GdHPDO3A (a compound approved for clinical practice).[12,13] As far as contrast enhancement is concerned, the internalization of CAs within endosomal vesicles may be an issue; as the exchange rate of water molecules across the endosomal membrane is slow, an unwanted "quenching" of relaxivity is observed at high concentrations of internalized Gd(III).[14,15] To avoid endosomal segregation, several procedures have been explored, including electroporation[14] or conjugation of the CAs with polyarginine based peptides as membrane penetrating

*To whom correspondence should be addressed. Phone: + 39 011 6706451. Fax: + 39 011 6706487. E-mail: silvio.aime@unito.it.

[a] Abbreviations: EPTs, exofacial protein thiols; MRI, magnetic resonance imaging; NMRD, nuclear magnetic relaxation dispersion; CA, contrast agent; DO3A, 1,4,7,10-tetraazacyclododecane-1,4,7-triacetic acid; DTPA, diethylenetriamine-*N*,*N*,*N*′,*N*′,*N*″-pentaacetic acid; P2T, pyridine-2-thione; DTNB, 5,5′-dithio-bis(2-nitrobenzoic acid); NEM, *N*-ethylmaleimide; TFA, trifluoroacetic acid; DCC, *N*,*N*′-dicyclohexylcarbodiimide; HEPES, 4-(2-hydroxyethyl)piperazine-1-ethanesulfonic acid; EBSS, Earl's balanced salt solution.



Published on Web 06/09/2010

**Scheme 1.** Structure and Reactivity of the GdDO3A and the GdDTPA Based Probes for the Labeling of EPTs

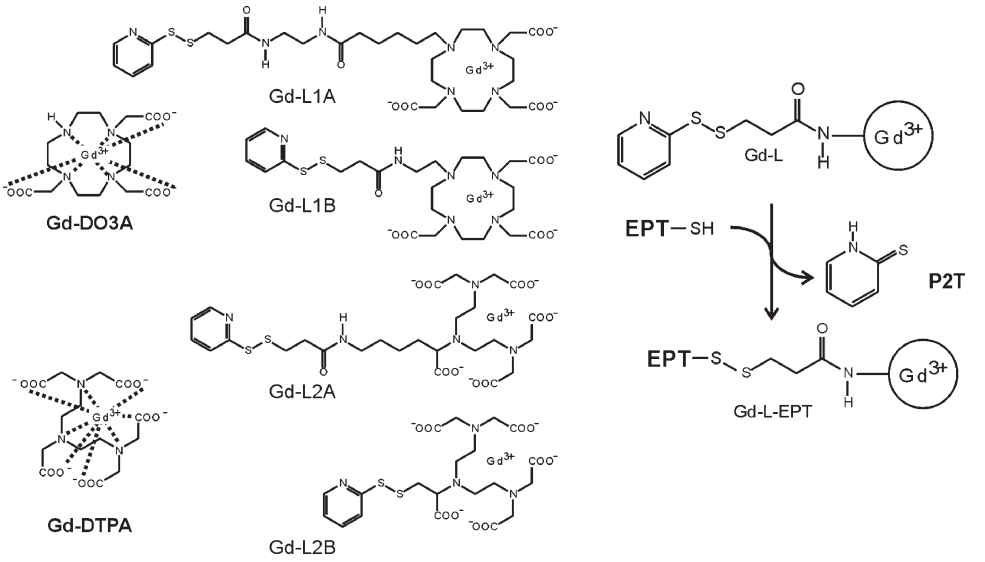


vectors.[16] An alternative concept to avoid the relaxivity "quenching" associated with endosomal entrapment is that of anchoring the imaging reporter on the extracellular side of the cell membrane rather than pursuing its internalization. This has been achieved, for instance, by forming a supramolecular adduct between the cell, a cationic polyarginine peptide, and the contrast agents under the form of negatively charged micelles.[17] Whatever the labeling strategy is, the minimum amount of Gd(III) complexes to be delivered to cells for MRI detection can be estimated by the following rule: $(r_1)(N) > 10^9$, where $N$ is the number of Gd(III) complexes per cell and $r_1$ is the actual relaxivity ($mM^{-1}\ s^{-1}$) of the Gd(III) complexes within the cellular environment.[5]

Recently we have undertaken a new method for labeling cells with Gd(III) based CAs exploiting the chemical reactivity of protein thiols that are exposed on the outer surface of cell membranes.[18] The imaging probe we have first synthesized[19] (GdL1A in Scheme 1, alias of Gd-DO3AS-Act in ref 18) is composed of a Gd(III) chelate, a reactive moiety for the recognition of thiols based upon the 2-pyridyldithio function, and a flexible linker connecting them. This probe can bind to exofacial protein thiols (EPTs) through a covalent disulfide bridge, leading to a satisfactory level of labeling in human myeloid leukemia K562 cell line. The proposed labeling procedure can be thought as being quite general, as it is known that several cell types express EPTs at sufficiently high levels: for instance, the concentration of EPTs is in the range 9−62 nmol·SH/$10^6$ cells for Chinese hamster ovary (CHO) cells,[20] 4−15 nmol·SH/$10^6$ cells for lymphocytes,[21] 15−30 nmol·SH/$10^6$ cells for human fibrosarcoma (HT1080) cells.[22] EPTs in these cells are reactive toward several chemicals, forming either reversible adducts (mixed disulfides) or irreversible adducts (thio ethers by coupling with maleimide derivatives or iodoacetamide derivatives).[23,24]

The purpose of this work is to clarify some aspects underlying the mechanism of EPT mediated cell labeling and assess the molecular properties of the labeling probes that play key roles for efficient labeling. Therefore, four probes based on either the DO3A chelate or the DTPA chelate and differing in the length of the spacer connecting the Gd(III) chelate with the thiol reactive unit have been synthesized, characterized, and evaluated for labeling efficacy (Scheme 1). The proposed labeling method has finally been applied to cells other than human myeloid leukemia K562 cells, initially chosen as a model system, to test the broad range application of this method.

## Results

**Synthesis of the Paramagnetic Probes.** Ligand L1A has been synthesized according to the route shown in Scheme 2. The spacer designed to connect the activated disulfide group with the DO3A-like chelating cage was synthesized by reacting *N*-(benzyloxycarbonyl)-1,2-diamineethane with 6-bromohexanoyl chloride, and the product (compound **1**) was purified. Compound **1** was then added dropwise to a solution of DO3A-tris-*tert*-butyl ester in acetonitrile to obtain compound **2**, which was purified by flash chromatography on silica. The cleavage of the benzyloxycarbonyl group has been achieved by hydrogenation with Pd/C at atmospheric pressure and room temperature to yield the free primary amino group, which was finally reacted with 3(2-pyridyldithio)propionic acid **4** in the presence of DCC. After removal of the *tert*-butyl ester protecting groups by treatment with trifluoroacetic acid, the compound was carefully purified to >98% by liquid chromatography on Amberlite XAD1600. Ligand L1B was synthesized starting from *N*-(benzyloxycarbonyl)-2-bromoethylamine (**13**) (the latter prepared from reaction of 2-bromoethylamine and benzyl chloroformate in water at pH 7) and DO3A-tris-*tert*-buthyl ester in acetonitrile. Hydrogenation to remove the benzyloxycarbonyl group, coupling to **4**, and deprotection of the carboxyl groups on the DO3A chelating cage were carried out essentially as for L1A. Ligand L2B, based on the DTPA chelating cage, was synthesized according to the route in Scheme 3. Compound **8** ($BF_3$ salt) was synthesized by reacting L-cysteine with aldrithiol in ethyl acetate in the presence of $BF_3$ ether ethylic complex. The primary amine was then dialkylated with **9** to give **10**, which was purified by flash chromatography on silica. Compound **11** (i.e., ligand L2B), obtained after deprotection of the carboxylic groups with TFA, was, however, not stable in water. HPLC chromatograms done at increasing time lapses after dissolution of L2B in water (at basic, neutral, and acidic pH) revealed

**Scheme 2.** Synthesis of the DO3A Based Probes GdL1A and GdL1B

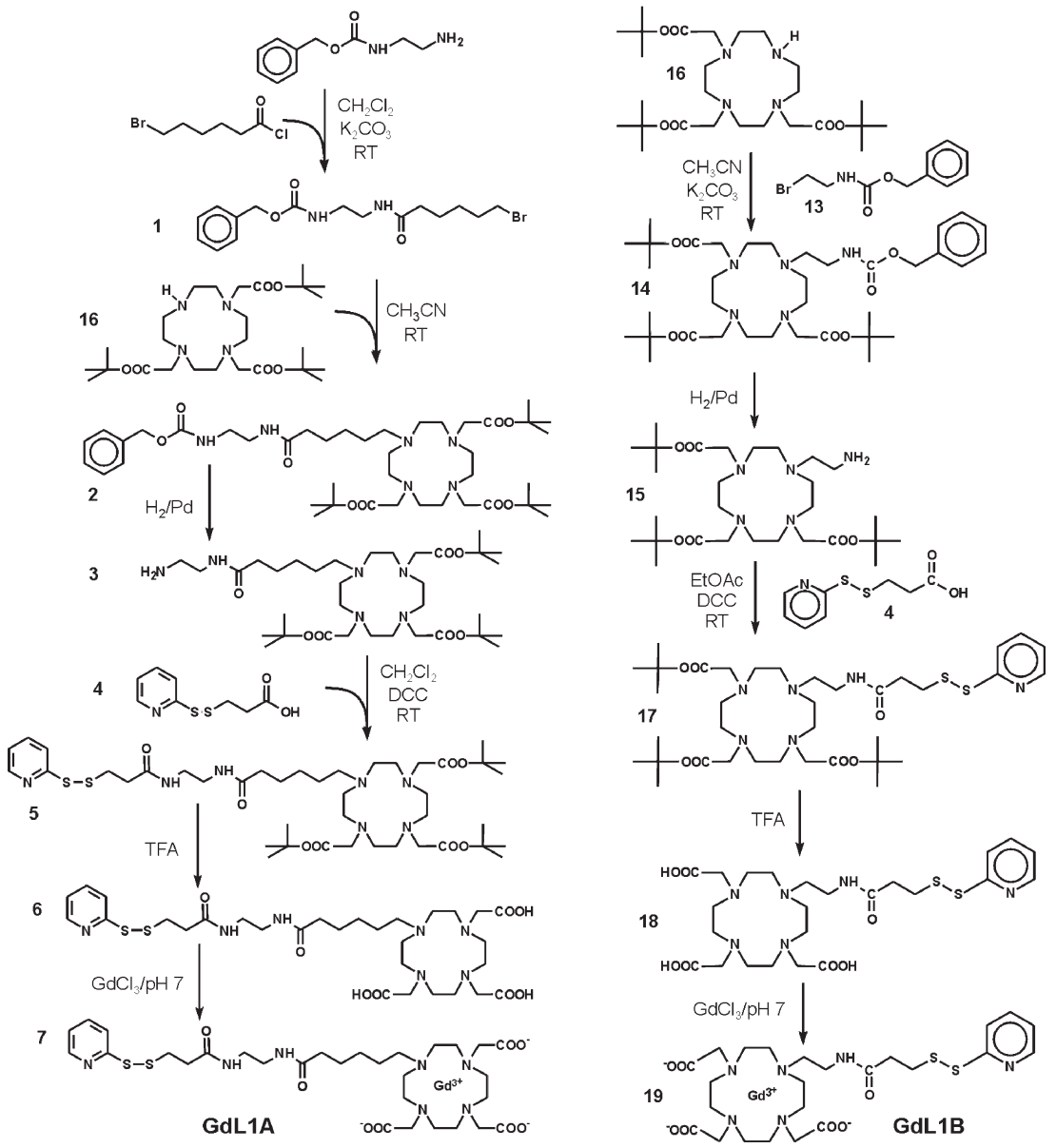


that the compound progressively released 2-pyridylmercaptane. For this reason the complexation of L2B with Gd(III) was performed very quickly on a freshly prepared aqueous solution of the ligand (pH 7) by adding $GdCl_3$ (0.95 equiv). The solution containing the complex was immediately freeze-dried. Unlike the free ligand, the GdL2B complex was stable in water. HPLC analysis of a solution of GdL2B in water (pH 7, room temperature) showed no formation of 2-pyridylmercaptane within 2 weeks. The DTPA-like L2A ligand was synthesized starting from **4** and **20**, whose synthesis has been described elsewhere.[25] The product **21** was purified by liquid chromatography on silica and deprotected with TFA. Unlike L2B, ligand L1B is stable in water. The complexation with Gd(III) of all ligands has been done according to the method described in ref 11, allowing a slight excess of the ligand (typically 2−3%) to ensure that all Gd(III) is under the complexed form, as free gadolinium is known to be readily taken up by cells.[26] The orange xylenol test[27] confirmed complete complexation of Gd(III).

**$^1$H and $^{17}$O NMR Relaxometric Characterization of the Probes.** The most relevant parameter summarizing the efficacy of a Gd(III) complex as a contrast agent (CA) for MRI applications is the millimolar relaxivity ($r_1{}^{mM}$, $mM^{-1}\ s^{-1}$), defined as the enhancement of the relaxation rate of solvent water protons promoted by the paramagnetic complex at 1 mM:

$$R_{1obs} = R_{1p} + R_{1w} \quad (1)$$

$$R_{1p} = r_1{}^{mM}[CA] \quad (2)$$

In these formulas proton longitudinal relaxation rates $R_1$ ($s^{-1}$) are related to longitudinal relaxation times $T_1$ (s) by the relationship $R_1 = 1/T_1$. $R_{1obs}$ is the measured water proton relaxation rate, $R_{1p}$ the paramagnetic enhancement to the water proton relaxation rate, $R_{1w}$ the relaxation rate of pure water, and [CA] the concentration of the Gd(III) complex in mmol/L. The higher the millimolar relaxivity, the better the ability of a given compound to enhance image contrast, other conditions being equal. Although the physicochemical factors

**Scheme 3.** Synthesis of the DTPA Based Probes GdL2A and GdL2B

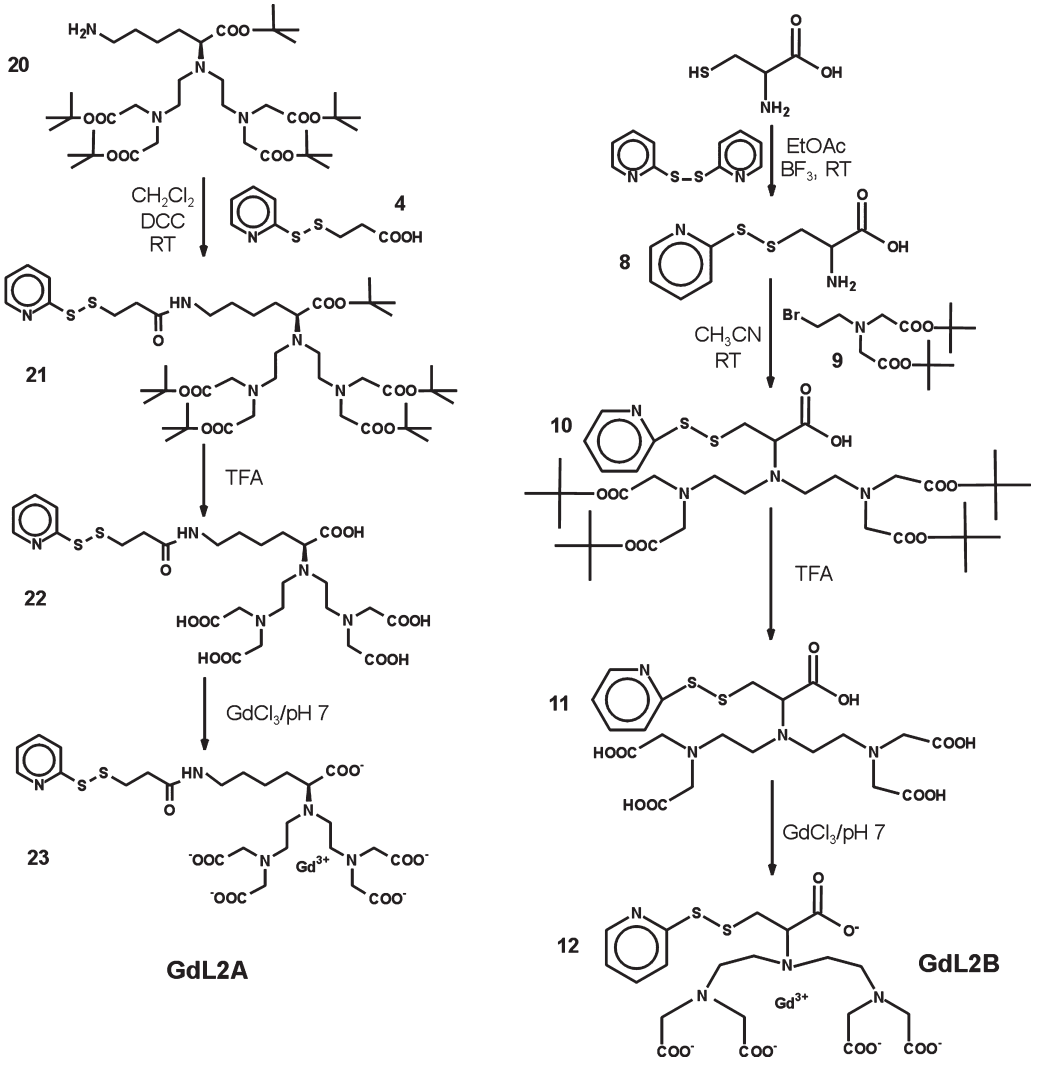


contributing to the relaxivity of a given compound are numerous and the theory governing them rather complex,[28,29] the differences between the relaxivities of chemically homogeneous Gd(III) chelates can be explained at a first approximation in terms of three fundamental parameters, namely, (i) the hydration number $q$, describing how many water molecules are directly coordinated to the metal center (inner sphere water molecules); (ii) the mean water residence lifetime $\tau_M$, describing the exchange dynamics of inner sphere water molecules with bulk water; and (iii) the reorientational correlation time for molecular tumbling $\tau_R$, describing the overall rotational tumbling motions of the molecule.

Table 1 lists the millimolar relaxivities of the four complexes in different environments, together with the relaxivity of parent GdDO3A and GdDTPA.[9] The relaxivities of the DTPA-based complexes (GdL2A, GdL2B) are very similar to each other and larger than that of parent GdDTPA because of the increased molecular size due to the introduction of the functionalizing moieties ($\tau_R$ effect). These relaxivities fall well within the range typical for low molecular weight GdDTPA based structures and are well consistent with $q = 1$ for both GdL2A and GdL2B. In comparison, the relaxivities within the GdDO3A-based compounds (GdL1A, GdL1B, and parent GdDO3A) show a less straightforward behavior. Both GdL1A and GdL1B would be expected to have relaxivities higher than that of parent GdDO3A because of their larger molecular size and because of the faster water exchange kinetics typically observed for *N*-alkyl or *N*-aryl derivatives of GdDO3A.[30] However, only GdL1A shows the expected relaxivity increase with respect to GdDO3A, whereas the relaxivity of GdL1B is almost identical to that of GdDO3A. Nuclear magnetic relaxation dispersion (NMRD) profiles and $^{17}O$-$R_{2p}$ versus temperature profiles were then acquired (Figure 1), as the multiparametric fitting of such profiles according to the Salomon−Bloembergen−Morgan

**Table 1.** Millimolar Relaxivities ($mM^{-1}$ $s^{-1}$, 25 °C) of the Probes in Different Chemical Environments

| | HEPES buffer, pH 7.4 | | HEPES buffer, pH 7.4, with 20 mM lactate | | |
|---|---|---|---|---|---|
| | 20 MHz | 300 MHz | 20 MHz | 300 MHz | K562 cell pellets 300 MHz |
| DO3A | 6.0[a] | 5.4 | 3.5 | 2.2 | |
| GdL1A | 9.0 | 7.4 | 3.0 | 2.6 | 2.0 |
| GdL1B | 6.3 | 5.9 | 3.1 | 2.5 | 2.3 |
| DTPA | 4.7[b] | 4.0 | | | |
| GdL2A | 6.7 | 5.8 | | | |
| GdL2B | 6.9 | 5.7 | | | |

[a] See also ref 31. [b] Taken from ref 9.

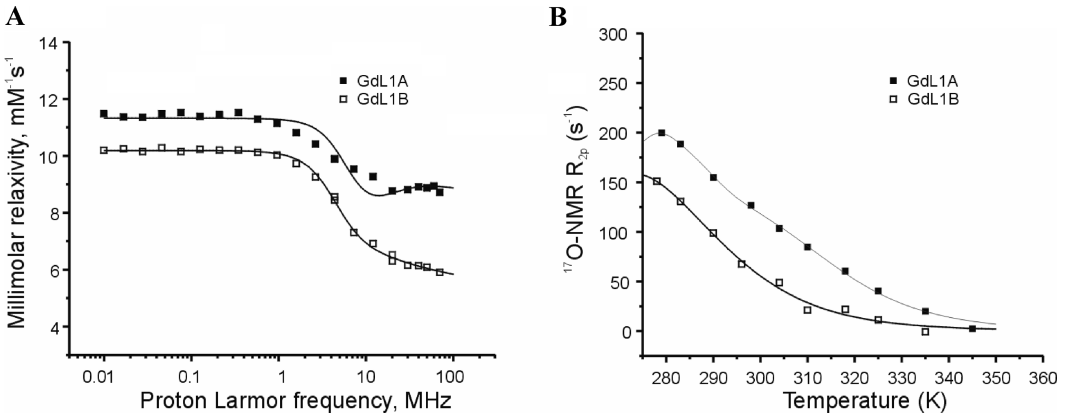


**Figure 1.** (A) $^{1}$H NMRD profiles of GdL1A (solid squares) and GdL1B (open squares): probe concentration of 1.0 mM, HEPES buffer, pH 7.4, 25 °C. (B) $^{17}$O-$R_{2p}$ versus temperature profiles of GdL1A (solid squares) and GdL1B (open squares): probe concentration of 5 mM, HEPES buffer, pH 7.4, 14.2 T. The solid lines represent best fit curves according to the Solomon−Bloembergen−Morgan theory with parameters reported in Table 2.

**Table 2.** Relaxation Parameters for GdL1A and GdL1B Obtained after Fitting of the NMRD and $^{17}$O-$R_{2p}$ versus $T$ Profiles[a]

| | $q$ | $\tau_m$ (ns) | $\tau_R$ (ps) | $\tau_v$ (ps) | $\Delta^2$ (s$^{-2}$) | $\Delta H_m$ (kJ mol$^{-1}$) |
|---|---|---|---|---|---|---|
| GdL1A | 2.0 | 28 | 113 | 22 | $6.2 \times 10^{19}$ | 59 |
| GdL1B | 1.1 | 13 | 110 | 29 | $2.8 \times 10^{19}$ | 66 |

[a] NMRD profiles were analyzed following Solomon−Bloembergen−Morgan theory for the inner-sphere relaxivity and the Freed model for the outer-sphere relaxivity (see text), fixing the diffusion coefficient ($D$) at $2.24 \times 10^{5}$ cm$^2$ s$^{-1}$, the distance between $Gd^{3+}$ and the inner sphere water protons ($r$) at 3.1 Å, and the distance of closest approach of outer-sphere water protons at 3.8 Å. $^{17}$O-$R_{2p}$ versus $T$ profiles were analyzed according to the Swift and Connick equation by fixing the distance between $Gd^{3+}$ and the inner sphere water oxygen (fixed to the values determined from $^{17}$O-$R_{2p}$ versus $T$ profiles of the complexes) at 2.5 Å and the Gd−$^{17}$O scalar coupling constant (A/ħ) at $-3.8 \times 10^{6}$ rad s$^{-1}$.

theory of paramagnetic relaxation[28] can give a more quantitative picture of the contribution of each relaxation parameter to the observed relaxivity. The most relevant outcome of such analysis (Table 2) is that, unlike GdL1A or GdDO3A both having $q = 2$, GdL1B is characterized by $q = 1$. The lower hydration can be explained by considering that the spacer arm in GdL1B can fold to coordinate the Gd(III) center, likely through the oxygen atom belonging to the amide group. In doing so, one of the two inner sphere water molecules that typically resides on the paramagnetic center in DO3A based complexes is displaced,[31] resulting into a lower hydration. The quantitative analysis of the temperature dependence of transverse relaxation rate ($R_{2p}$) of the metal bound $^{17}$O water resonance (Figure 1B) is considered the method of choice for the evaluation of the exchange lifetime of the coordinated water molecule(s) ($\tau_M$).[32,33] In the case of both the DO3A derivatives considered in this study, very short $\tau_M$ values have been determined, namely, 28 and 13 ns for GdL1A and GdL1B, respectively. These values are in the range of optimal values for the attainment of very high relaxivity once the molecular tumbling of the system is lengthened as a consequence of the formation of a macromolecular adduct.[34] The difference in the amplitude of the two profiles reported in Figure 1B (GdL1A shows $^{17}$O-$R_{2p}$ values higher than those of GdL1B) is a consequence of the higher hydration number of GdL1A with respect to GdL1B.

The Gd(III) ion in DO3A based structures can establish coordinative bonds with anions (such as carboxylates) other than those strictly belonging to the DO3A cage, leading to the formation of ternary complexes characterized by their

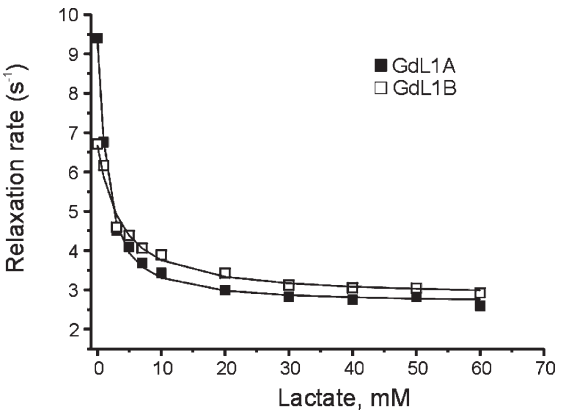


**Figure 2.** Titration curves of GdL1A (solid squares) and GdL1B (open squares) with lactate (0.47 T, HEPES buffer, pH 7.4, 25 °C). The lines represent the best fitting of the curve according to the model described in ref 37, from which the association constants ($K_a$) and the millimolar relaxivities of the ternary complexes ($r_1^{bound}$) can be extracted.

own relaxation properties.[35,36] In this article it will become clear that the formation of such a ternary complex has important implications for the understanding of the EPT dependent labeling mechanism. Therefore, we provide here the characterization of the interaction between the DO3A based probes and foreign carboxylates, such as lactate. The 0.5 mM solutions of either GdL1A or GdL1B have been added with increasing amounts of lactate, which is known to have a good affinity for GdDO3A and related compounds.[37] The observed water proton relaxation rate $R_{1obs}$ decreases as the concentration of lactate increases (Figure 2) because the coordination of Gd(III) by lactate decreases the hydration at the paramagnetic center. By fitting of the titration curve to the model described in ref 37, the association constants ($K_a$) and the relaxivity of the GdL1A/lactate and GdL1B/lactate ternary complexes ($r_1^{bound}$) could be extracted. Association constants of $1000 \pm 60$ M and $330 \pm 40$ M for GdL1A and GdL1B, respectively, were found. The slightly higher affinity of GdL1A with respect to GdL1B for lactate is likely due to the fact that lactate binding in GdL1B partially competes with intramolecular self-coordination by the functionalized arm. The relaxivities $r_1^{bound}$ of the ternary complexes were 2.3 and 2.4 mM$^{-1}$ s$^{-1}$ for GdL1A and GdL1B, respectively,

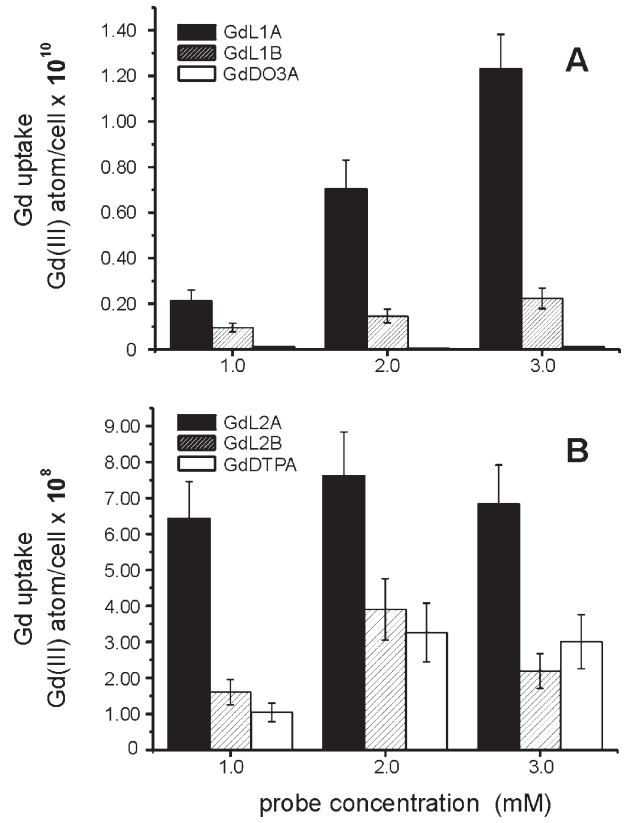


**Figure 3.** Uptake of Gd(III) chelates (expressed as Gd(III) atoms per single cell) by K562 cells as a function of the concentration of the probes in the incubation medium (4 h, 37 °C): (A) GdDO3A based probes (GdL1A/GdL1B) with GdDO3A as the control; (B) GdDTPA based probes (GdL2A/GdL2B) with Gd-DTPA as the control. Note that the scaling of the *y*-axis in panels A and B differs by 2 orders of magnitude, pointing out the much higher labeling efficacy of the GdDO3A based probes compared to the GdDTPA based counterparts.

indicating that these complexes essentially behave as outer sphere systems (i.e., they have no inner sphere water molecules). This is due to the fact that lactate behaves as a bidentate ligand, displacing both water molecules from the Gd(III) center.[37] In summary, GdL1A and GdL1B have $q = 2$ and $q = 1$, respectively, unless they interact with carboxylates (or other coordinating anions) to form ternary complexes characterized by the absence of inner sphere water molecules. The interaction of GdDO3A-like complexes with further anions is favored by the formal neutral net charge in the complex and by the fact that the DO3A chelating cage is heptadentate, leaving two easily accessible coordination sites free on the Gd(III) center.

**Labeling of K562 Cells.** Preliminary to cell labeling with Gd(III) chelates, the concentration of EPTs on K562 cells has been assessed through the DTNB assay.[18,20] The number of DTNB-titrable EPTs is in the range $(5.0-18.0) \times 10^9$ EPTs/cell, depending on the cell density in culture flasks (see Supporting Information Figure S1). In typical cell labeling experiments, 5 million K562 cells at a density of $1.5 \times 10^6$ cells/mL (displaying $(5-7) \times 10^9$ EPTs/cell) were incubated in a minimum medium (EBSS, Earl's balanced salt solution with HEPES buffer, thiol free) for 4 h at 37 °C in the presence of the probe (0.5−3.5 mM). At the end of the incubation period, cells showed a viability higher than 90%, indicating an overall good tolerability. Cells were then separated from

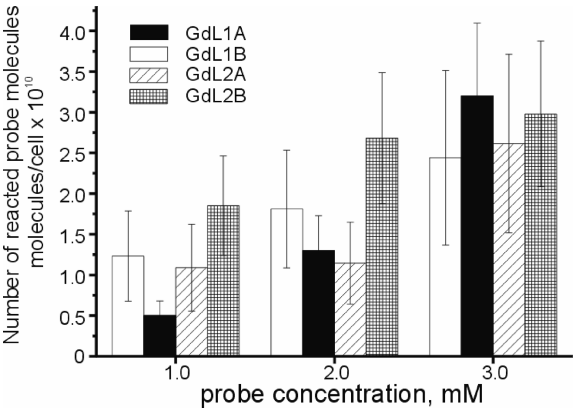


**Figure 4.** Amount of pyridine-2-thione (P2T) released during the incubation of K562 cells (4 h, 37 °C) with the probes, expressed as the number of released P2T molecules per single cell.

the incubation medium, pelleted, resuspended, and washed to remove as much as possible the unreacted or aspecifically bound probe and finally subjected to mineralization and quantitative analysis of Gd(III) by a relaxometric assay.[12,26] This experimental setup provides the measurement of the total amount of Gd(III) taken up by cells, which is plotted in Figure 3 as a function of the concentration of the probes in the incubation medium. Parent GdDO3A and GdDTPA were used as controls for GdL1A/GdL1B and GdL2A/GdL2B, respectively, to evaluate the level of Gd(III) uptake unrelated to the EPT chemistry. Among the DO3A-based probes, GdL1A shows by far the highest levels of Gd(III) uptake (as many as $1.2 \times 10^{10}$ Gd(III) atoms/cell), while GdL1B has a lower but still significant uptake (up to $2.2 \times 10^9$ Gd(III) atoms/cell). The relationship between the total amount of Gd(III) taken up by these two probes and the concentration of the probe in the incubation medium is approximately linear. No plateau is observed at the higher probe concentrations, indicating that EPTs binding sites are not saturable. On the other hand, the DTPA-based probe GdL2A showed a barely detectable uptake, whereas GdL2B did not show any significant uptake, neither in absolute terms nor in comparison with parent GdDTPA as the control (Figure 3B).

To gain further insight into the cause of the large differences in the uptake of the DO3A-based and DTPA-based probes, the ability of each of the complexes to target EPTs was evaluated by UV−vis spectrophotometry. When the probes react with EPTs to form a disulfide bridge, pyridine-2-thione (P2T) is released as a byproduct (Scheme 1) in the incubation medium and it absorbs light at 343 nm. Therefore, the increase in $A_{343}$ from the start of the incubation to the end of the incubation gives an estimate of the amount of probe that has reacted with EPTs. Figure 4 shows that the amount of P2T released increases linearly with the concentration of the probe in the medium, with little (if any) differences between the four probes, indicating that all probes react with EPTs with similar reaction yields. Interestingly enough, the release of P2T is uncorrelated with Gd(III) uptake by cells. The DO3A-based probes react with EPTs and are taken up by cells, whereas the DTPA-based ones are poorly or not taken up at all while reacting with EPTs to the same extent as the DO3A-based counterparts do. Therefore, the different efficiency of cell labeling shown by the two probe families cannot be explained on the basis of a different reactivity toward EPTs. Finally we note that for

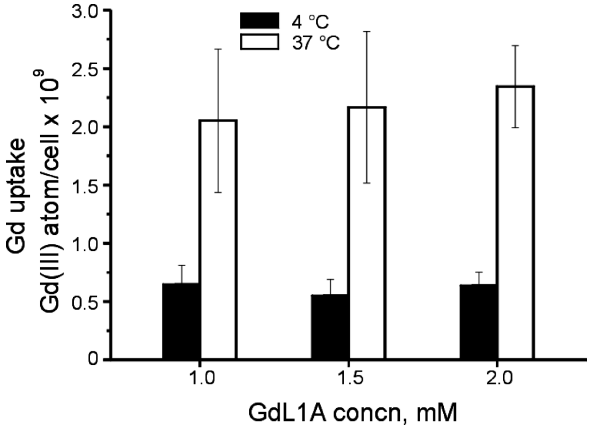


**Figure 5.** Uptake of GdL1A (Gd atoms/cell) by K562 cells as a function of the concentration of GdL1A in the incubation medium (1 h incubation): white, labeling carried out at 37 °C; black, labeling carried out at 4 °C.

GdL1A, showing the best labeling efficiency, the amount of reacted probe per single cell is about 3 times larger than the amount of Gd(III) units found in cells, indicating that only one-third of the reacted probe is taken up by cells.

To assess whether active cellular mechanisms were involved in the labeling with GdL1A, labeling experiments were carried out at 4 °C, where most of the active transmembrane transport systems are inhibited. The extent of labeling at 4 °C was then compared with that obtained in parallel experiments carried out at 37 °C (Figure 5). In this set of labeling experiments, the incubation time was shortened to 1 h to minimize cell suffering due to the low temperature. At the lower temperature, the amount of gadolinium taken up by cells is apparently constant within the probe concentration range, with an average value of around $6 \times 10^8$ Gd(III) atoms/cell, and about 60% lower than the amount of gadolinium that is taken up at 37 °C. Because of the short incubation time (1 h), uptake of GdDO3A at both 37 and 4 °C is below the detection limit of the relaxometric assay, estimated to be $1 \times 10^8$ Gd(III) atoms/cell for this set of experiments. It must be emphasized that the difference in Gd(III) uptake at the two temperatures cannot be ascribed to temperature effects on the reactivity of GdL1A with EPTs at 37 °C compared to that at 4 °C, as the release of P2T at 4 and 37 °C was comparable. These findings clearly indicate that active cellular processes are at least partially involved in EPTs-mediated cell labeling, likely yielding the internalization of substantial amounts of the Gd(III) containing probes. It must be emphasized that gadolinium in cells labeled with GdL1A is present under the form of the intact complex and that the dissociation of Gd(III) ions from the DO3A chelating cage to yield "free gadolinium" is negligible, as demonstrated in a previous study.[18]

**Relaxivity of the DO3A-Based Probes in the Cellular Environment.** The different degrees of cell labeling achievable by the compounds considered in this work can be qualitatively appreciated by $T_1$-weighted spin−echo MR images (7.0 T) of labeled cell pellets. Figure 6A shows some representative images, where cells labeled with GdL1A or GdL2A have been dispersed into agar phantoms (representative images with GdDO3A are given in Supporting Information Figure S2). GdL1A produces a 7-fold or a 5-fold signal enhancement with respect to unlabeled cells, corresponding to concentrations of the probe in the labeling medium of 2 or

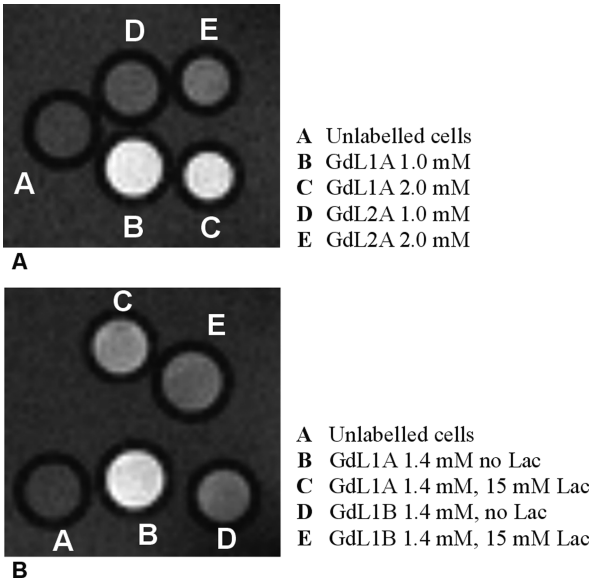


**Figure 6.** (Part A) $T_1$-weighted spin−echo images (measured at 7 T) of agar phantoms containing K562 cell pellets: (A) control (unlabeled) cells; (B, C) cells labeled with 1.0 and 2.0 mM GdL1A, respectively; (D, E) cells labeled with 1.0 and 2.0 mM GdL2A, respectively. (Part B) Effect of lactate added to the labeling medium on cell labeling: (A) control cells; (B, C) cells labeled with GdL1A (1.4 mM) without and with lactate 15 mM, respectively; (D, E) cells labeled with GdL1B (1.4 mM) without and with lactate 15 mM, respectively. See Supporting Information Figure S2 for MR images of cells labeled with control GdDO3A.

1 mM, respectively. For compound GdL2A, showing minimal levels of uptake, a 2-fold signal enhancement becomes detectable when labeling is carried out with a probe concentration of 2 mM.

To assess the millimolar relaxivity $r_1^{mM,cell}$ of the complexes within the cellular environment, proton relaxation rates were measured on a series of cell pellets labeled with increasing concentration of the probes and the values normalized by the total content of gadolinium in the cells ($Gd_{cell}$) and by the volume of cells. To this purpose, 5 million cells were labeled with increasing concentrations of GdL1A or GdL1B (0.5−5 mM, 37 °C, 4 h), washed, and centrifuged, the supernatant was carefully removed, and cells were dispersed into agar phantoms. After the measurement of the water proton relaxation rate $R_{1obs}$ by means of the saturation−recovery spin−echo pulse sequence, pellets were recovered and analyzed for the total gadolinium content. These measurements yielded millimolar relaxivities in cell of 2.0 and 2.3 $mM^{-1} s^{-1}$ (at 7.0 T, 25 °C) for GdL1A and GdL1B, respectively (Table 1). These quite similar values confirm that the difference in the signal enhancement between cells labeled with GdL1A and GdL1B is due to the differential uptake of the two probes rather than to differences between their relaxivities in the cellular environment.

The graph plotting $R_{1obs}$ versus the content of gadolinium per cell ($Gd_{cell}$, Gd(III) atoms/cell) can be further worked out to gain insights into the cellular compartmentalization of the Gd(III) complexes. This graph (Figure 7) also contains data taken from the literature relative to the labeling of hepatocarcinoma HTC cells with GdHPDO3A,[14] a contrast agent in clinical use. GdHPDO3A has been used to label cells through the electroporation or the pinocytosis techniques. GdHPDO3A is known to be internalized by both methods,

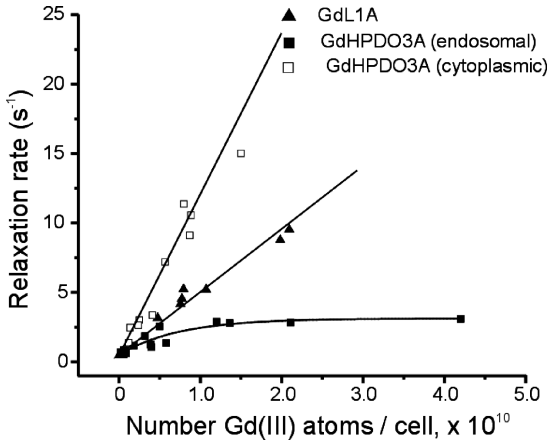


**Figure 7.** Observed water proton relaxation rates $R_{1obs}$ of cell pellets (about 5 millions cells, 25 °C) that have taken up different amounts of gadolinium complexes: (solid triangles) K562 cells (this work) labeled with GdL1Ap; (open squares) HTC cell pellets labeled with GdHPDO3A (taken from ref 14) through electroporation, leading to cytosolic localization; (solid squares) HTC cell pellets labeled with GdHPDO3A through pynocytosis, leading to endosomal entrapment (taken from ref 14). Best fit straight lines are shown for the open square and triangles data points. The curve through the solid squares is drawn only to guide the eye and to highlight the plateau effect that is typical of compartmentalization of Gd(III) chelates into poorly water-permeable cell substructures.

but its distribution within the cell is different. If internalization is achieved through the electroporation method, GdHPDO3A resides mostly in the cytoplasm or, more strictly, it is not compartmentalized within subcellular organelles delimited by poorly water permeable membranes. Noncompartmentalized internalization of GdHPDO3A results in a linear relationship between $R_{1obs}$ and the content of gadolinium per cell, as there are no limitations due to slow water exchange between intracellular compartments and the extracellular space (Figure 7, open squares). On the other hand, if GdHPDO3A uptake occurs through pinocytosis, the complex is compartmentalized into membrane-delimited vesicles that limit the exchange of water between the intravesicle environment, the cytoplasm, and the extracellular space. A rather complex three-site exchange model is required to describe relaxation. In this case a relaxivity "quenching" effect is observed, resulting in a plateau in the $R_{1obs}$ versus $Gd_{cell}$ plot at a $Gd_{cell}$ of $2 \times 10^9$ Gd(III) atoms/cell (Figure 7, solid squares). The functional form of these curves is then related to the compartmentalization of Gd(III) complexes within the cell. When cells are labeled with GdL1A, a linear plot is observed up to a concentration of $3 \times 10^{10}$ Gd(III) atoms per cell, and no relaxivity quench is observed (Figure 7, triangles). This suggests that after internalization the GdL1A complex is not sequestered into subcellular organelles.

**Effect of the Concentration of EPTs on Cell Surface on the Uptake.** GdL1A, showing the best labeling efficacy, has been used to label K562 cells displaying different levels of EPTs to gain further insights into the link between the number of available EPTs and the Gd(III) uptake. To this purpose, cells were treated with chemicals known to block EPTs prior to the incubation with the labeling agents. NEM has been chosen as the thiol blocking compound because it can form irreversible thioether bonds with EPTs, it is relatively well tolerated by cells, and it cannot cross cell membranes.[24] The efficacy of NEM in decreasing the number of available EPTs has been evaluated by incubating K562 cells with NEM (0.1−1 mM, 4 °C, 15 min) and then by titrating the amount of residual EPTs by the DTNB spectrophotometric assay (i) immediately after the treatment with NEM and (ii) after an additional incubation time (recovery time) of 3 h at 37 °C in minimal culture medium (data not shown). At the maximum concentration of NEM (1 mM), cells showed a viability larger than 80% (trypan blue test) in both circumstances. The number of available EPTs measured immediately after 1.0 mM NEM treatment decreases by a factor of 5 with respect to control, whereas the number of EPTs measured after the recovery time showed only a 2-fold decrease of EPTs, indicating that cells are able to partially restore the functionality of EPTs. Next, true labeling experiments were carried out by first pretreating cells with NEM (concentration range 0.1−1 mM, 4 °C, 15 min) to increasingly mask EPTs and then by incubating cells for 3 h at 37 °C with 2 mM GdL1A. Although cell viability is not significantly affected by any of the two single treatments (NEM at 4 °C or GdL1A at 37 °C), the catenation of the two resulted in a severe increase in cell death. Only pretreatment with the lower concentration of NEM (0.1 mM) resulted in a viability of > 80% at the end of the whole labeling experiment. The decrease of Gd(III) uptake between control and cells pretreated with 0.1 mM NEM was ~45% (data not shown). These results clearly indicate a direct proportionality between the amount of probe taken up and the concentration of available EPTs on cells.

**Effect of Lactate on the Uptake of DO3A-Based Probes.** Since the DO3A-based probes are taken up by cells while the DTPA-based ones are not, the characteristics of the metal chelate must play a major role in the uptake mechanism. This is quite unexpected, as the targeting to the EPTs in the original design of the probes relied entirely on the thiol reactive 2-pyridyldithio unit. The role of the metal chelate might be related to the differences between GdDTPA and GdDO3A-based complexes in terms of net charge and possibility to establish further coordination with foreign carboxylates or other anions. To assess whether the coordination chemistry at the Gd(III) center could have any effect on the labeling efficacy, labeling experiments with the DO3A-based probes have been carried in the presence of increasing concentrations of lactate in the incubation medium. As stated above, lactate can coordinate in a bidentate manner the Gd(III) center in GdL1A or GdL1B complexes and can form ternary complexes with dissociation constants in the millimolar range. Figure 8 shows that the total amount of both GdL1A and GdL1B (1.5 mM, 37 °C, 4 h) taken up by cells decreases proportionally with the concentration of lactate added in the incubation medium. In the case of GdL1A, the percentage inhibition is particularly striking: as much as 73% when lactate concentration is 15 mM (in these conditions, the molar concentration of free GdL1A with respect to the GdL1A/lactate ternary complex is about 5%). The millimolar relaxivity of cell pellets labeled with GdL1A in the presence or absence of lactate does not change appreciably. The decrease of signal enhancement in cell pellets labeled in the presence of lactate (Figure 6B) is entirely due to a lower concentration of gadolinium taken up by the cells.

**Labeling of C6 and B16 Cells.** To probe the range of applicability of the proposed labeling procedure, it has been applied to rat glioma (C6) and murine melanoma (B16) cultured cells. The latter cell types grow in adhesion to the culture vessel and may offer a lower availability of EPTs to the labeling probes compared to K562 cells, which grow as

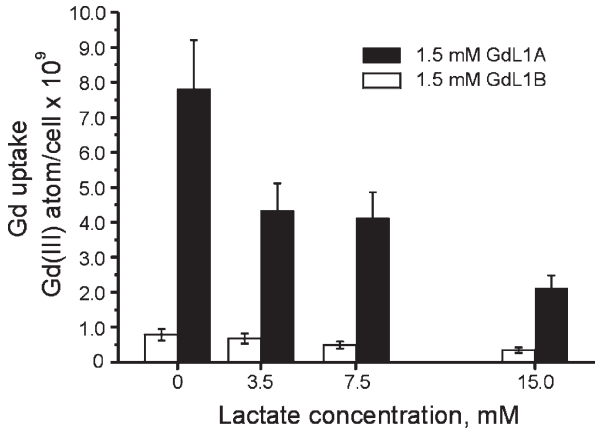


**Figure 8.** Uptake of GdL1A (Gd(III) atoms/cell) by K562 cells as a function of the concentration of lactate in the incubation medium (4 h of incubation, 37 °C, about 5 millions cells): white bars, cells labeled with GdL1B; black bars, cells labeled with GdL1A.

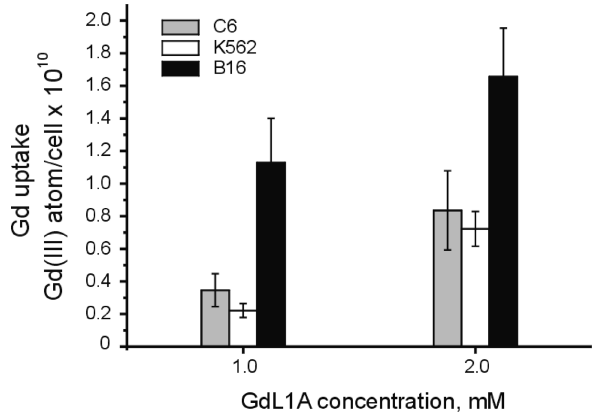


**Figure 9.** Extent of cell labeling (expressed as Gd(III) atoms/cell) by GdL1A as a function of the concentration of GdL1A in the labeling medium (about $5 \times 10^6$ cells, 37 °C, 4 h): rat glioma C6 (gray bars); human myeloid leukemia K562 (white bars); murine melanoma B16 (black bars). See Supporting Information Figure S3 for control uptake of GdDO3A.

suspended cells. The level of EPTs expressed by C6 and B16 cells (measured at a confluence of 80%) was $(2-4) \times 10^9$ and $(2-6) \times 10^{10}$ EPTs/cell, respectively, by the DTNB spectrophotometric assay, whereas the level of EPTs/cell is in the range $(5-7) \times 10^9$ for K562 cells. For labeling, cells grown to a confluence of 80% were subjected to a 4 h incubation with 2 mM GdL1A at 37 °C, washed three times, and detached from the flasks by treatment with trypsin. As shown in Figure 9, a good labeling could be obtained for all cell lines, with a minimum labeling of $1 \times 10^9$ Gd(III) atoms/cell (data for control GdDO3A in Supporting Information Figure S3). The higher efficacy of the labeling on B16 cells with respect to C6 and K562 correlates well with the higher level of EPTs shown by the former.

## Discussion

The original concept of cellular labeling through the bioconjugation of EPTs with a suitably activated paramagnetic probe relied upon the fact that cells display a large number of DTNB reactive EPTs (in the range of $(2-60) \times 10^9$ EPTs/cell for those considered in this work) that can be exploited as anchorage points for suitably activated probes. If as much as 10−25% (depending on cell type) of these EPTs could be labeled with Gd(III)-based probes having a millimolar relaxivity of 2 $mM^{-1}$ $s^{-1}$, each cell would be covered with a number of Gd(III) centers large enough to allow visualization by MRI. The necessity of the formation of a covalent EPT−probe adduct for labeling is well pointed out by the fact that the chemical blockage of EPTs by NEM considerably decreases the extent of labeling. Moreover, the extent of labeling is proportional to the concentration of EPTs available on cells. On the other hand, the fact that all of the probes considered do react with EPTs while showing widely different labeling properties (maximum efficiency for GdL1A, no labeling at all for GdL2B) clearly indicates that the formation of the EPT−probe adduct is not sufficient by itself for labeling cells to a suitable extent. Thus, the EPT-dependent labeling mechanism goes beyond the simple anchorage of the probes on the extracellular side of the plasma membrane, and the fate of the EPTs−probe adduct must be taken into account. More detailed labeling experiments performed with GdL1A, the best performing probe, revealed that (i) the total amount of Gd(III) taken up per single cell is significantly larger than the number of EPTs available on cells; (ii) the relationship between Gd(III) uptake and the concentration of the probe in the incubation medium is linear up to 3.5 mM probe concentration, where the stoichiometric ratio between the probe and the EPTs is largely in favor of the former (in these conditions, a saturation of the EPTs and a plateau in the Gd(III) uptake vs probe concentration graph would be expected, but it is not observed); (iii) labeling cells with GdL1A at 4 °C is about 60% less effective than that achieved at 37 °C, indicating that active cellular transport mechanisms, which are inhibited at 4 °C, must play a role and that some degree of probe internalization is involved.

Taken together, these findings provide evidence about the internalization of a substantial amount of the probe, which must take place upon cellular processing of the EPT−probe adduct. It may be envisaged that after the formation of the disulfide bridged EPT−probe adduct, the cell machinery comes into play to restore the physiological thiol/disulfide redox balance on the extracellular side of the plasma membrane. This balance has been shown to be essential for proper cell function, as exofacial protein thiols/disulfides may act as redox switches involved in many functions,[38] such as intracellular signaling, cell adhesion, or integrin activity.[23,39] As a matter of fact, cells have been shown to have several ways to buffer (at least partially) the exofacial protein thiol/disulfide redox state.[21,22,40] The cell response to the formation of the EPT−probe mixed disulfide could ultimately result into the cleavage of such an adduct (by reduction or by thiol/disulfide exchange), which can lead to either the ejection of the probe in the extracellular space or the internalization of the probe. Dealing with internalization, it becomes important to evaluate the chemical form of Gd(III) and its intracellular localization. In a previous work it has been proved that the GdL1A probe is present in the cell environment as the integer GdDO3A like complex and that the release of free Gd(III) from the DO3A cage is negligible.[18] Although we have no explicit data on the cellular localization of the internalized probe, the analysis of the plots linking the observed relaxivity of cell pellets as a function of the cellular concentration of gadolinium may provide some clues (Figure 7). It has been shown that the relaxivity increases linearly (up to a total concentration of gadolinium of $2 \times 10^9$ Gd(III) atoms/cell) when the internalized Gd(III) complex resides in the cytoplasm or, more

generally speaking, when it is not sequestered in poorly water permeable subcellular organelles. On the other hand, the relaxivity goes to a plateau when the complex is sequestered within cellular substructures such as the endosomes, where the exchange rate of water molecules between the intraorganelle and the cytoplasmatic compartments is so slow as to quench the paramagnetic relaxivity enhancement.[14] In the case under study, we found a linear relationship between the observed paramagnetic relaxivity and the total gadolinium content, up to a $Gd_{cell}$ concentration of $3 \times 10^{10}$ Gd(III) atoms/cell. This behavior suggests a noncompartmentalized cellular localization of the probe.

To assess the structural requirements favoring the internalization route of the probe, we compared the labeling efficacy of four probes differing either in the length of the spacer connecting the paramagnetic unit with the thiol binding unit or in the structure of the polyaminocarboxylic coordination cage (DO3A-like versus DTPA-like structures). These probes show wide differences in their cell uptake in the order GdL1A (maximum uptake) $\gg$ GdL1B $>$ GdL2A $\gg$ GdL2B (no uptake). This trend highlights that (i) DO3A-based probes are much more efficiently taken up than DTPA-based ones and (ii) within each of these two classes of compounds, uptake is favored by long, flexible spacers (GdL1A more easily taken up than GdL1B). The structure of the chelating cage is more important than the spacer length in defining the extent of uptake: the DO3A-based GdL1B, having a spacer slightly shorter than that of the DTPA-based GdL2A, still shows a better uptake. Although unplanned, the reporter moiety of the probes appears to play an active role in the EPT dependent labeling. A few remarks about the most important structural differences between GdDO3A-based and GdDTPA-based structures may help to shed light on such an unexpected role. GdDO3A-like complexes have a neutral net charge and typically two water molecules in the inner coordination sphere. With the DO3A-based structures being heptadentate and with their Gd(III) complexes being formally neutral, the GdDO3A complex can approach foreign negatively charged coordinating groups and make ternary complexes (for instance, with lactate, amino acids, protein carboxylates[19,30,37]), with the displacement of the inner sphere water molecules. On the other hand, DTPA-based structures are octadentate and their Gd(III) complexes have a doubly negative net charge, preventing the formation of ternary complexes with foreign coordinating groups. Typically, GdDTPA complexes have one inner sphere water molecule. The analysis of NMRD and $^{17}O$-$R_{2p}$ versus temperature profiles of GdL1A and GdL1B clearly shows that these compounds are characterized by $q = 2$ and $q = 1$, respectively, when they are in the free state, i.e., in the absence of potential foreign coordinating groups. The lower hydration of GdL1B is likely due to the further intramolecular coordination of the Gd(III) ion by the carbonylic oxygen belonging to the amido group of the spacer closer to the metal ion. In the presence of excess lactate, the hydration of both the DO3A-based probes decreases because of the formation of a ternary complex in which lactate acts as a bidentate ligand leading formally to the displacement of both inner sphere water molecules. Thus, in the presence of lactate, the GdDO3A moiety acquires one negative net charge and a lower hydration, quite resembling the GdDTPA structure. Consistently, the uptake of GdL1A or GdL1B in the presence of 15 mM lactate is strongly inhibited (by 73% and 56%, respectively). At present we are unable to state whether the key property for uptake is the formal neutral net charge of the Gd(III) chelate or the possibility of Gd(III) to form ternary complexes within the EPT−probe adduct (for instance, with exofacial protein carboxylates or membrane lipid phosphate headgroups as donors). Anyway, the formal charge of the complex and the coordination chemistry at the Gd(III) center are molecular properties that are strongly linked to each other. Finally, it is worth noting that the length/flexibility of the linker also has a role in determining the extent of labeling: the longer is the spacer, the higher is the amount of gadolinium taken up (compare GdL1A with GdL1B, Figure 3). In view that the formation of a ternary complex between the EPT-bound probe and some coordinating groups on the cell surface is important for internalization, a longer (and flexible) spacer would be beneficial because a longer spacer would allow a greater degree of freedom for the Gd(III) ion to probe the surface of the membrane protein (or the protein/membrane interface) in search of coordinating groups.

## Conclusions

We have described a new method for labeling cells with paramagnetic compounds based on the conjugation of GdDO3A-based complexes with exofacial protein thiols followed by the internalization of the probe. Suitable probes for this labeling scheme are GdDO3A-like molecules functionalized with the thiol reactive 2-pyridyldithio group through a long, flexible spacer. The proposed method can be thought of as being of quite general purpose, as reactive EPTs are present in a wide variety of cell lines. All three cell lines considered in this work could be successfully labeled for MRI visualization. In comparison to other methods for cell labeling with low molecular weight Gd(III) chelates the labeling procedure appears faster or less invasive, the payload of Gd(III) within cells being comparable. Segregation into intracellular vesicles or endosomes leading to relaxivity "quenching" is avoided.

## Experimental Section

The purity of every compound synthesized was determined through HPLC−UV and HPLC−ESI-MS by the ratio of the integrated HPLC peak area for the compound of interest to the integrated HPLC peak area for all peaks. For compounds GdL1A, GdL1B, GdL2A, and GdL2B the purity was $>95\%$.

**Synthesis of GdL1A. *N*-(Benzyloxycarbonyl)-*N*′-6-bromohexanoyl-1,2-diamineethane (1).** A solution of 6-bromohexanoyl chloride (14.0 g, 0.065 mol) in dichloromethane (100 mL) was added to *N*-(benzyloxycarbonyl)-1,2-diamineethane (12.6 g, 0.065 mol) and potassium carbonate (powder, 325 mesh,13.6 g, 0.10 mol) in dichloromethane (200 mL) at 0−5 °C under vigorous stirring. After 1 night at room temperature the solid was filtered and the solution washed with water, HCl 0.1 N, and brine. The clear solution was evaporated on a rotary evaporator to yield an oil (24.3 g).

**1-[5-[*N*-[2-[*N*-(Benzyloxycarbonyl)amine]ethyl]aminecarbonylpentyl]-1,4,7,10-tetraazacyclododecane-4,7,10-triacetic(1,1′-dimethylethyl ester) (2).** The free base of DO3A-tris-*tert*-butyl ester (**16**) was obtained by elution of DO3A·HBr with water/ethanol on Amberlite IRA 410). Compound **1** (18.5 g, 0.050 mol) was then added to a solution of DO3A-tris-*tert*-butyl ester (32.9 g, 0.064 mol) and *N*,*N*-diisopropylethylamine (8.3 g, 0.064 mol) in anhydrous acetonitrile (160 mL). After 4 days, the solution was evaporated on a rotary evaporator to yield an oil that was purified by flash chromatography on silica with a dichloromethane/methanol 20:1 v/v to remove the impurities and with pure methanol to recover the product (21.9 g).

**1-[5-[*N*-[2-Amineethyl]aminecarbonylpentyl]-1,4,7,10-tetraazacyclododecane-4,7,10-triacetic(1,1′-dimethylethyl ester) (3).** Compound **2** (20.9 g, 0.026 mol) was dissolved in methanol (60 mL), and 10% Pd/C (1.2 g) was added. Then the reaction was carried out under hydrogen atmospheric pressure at room temperature for 6 h. The mixture was then filtered and the solvent evaporated to yield an oil (17.3 g).

**3-(2-Pyridyldithio)propanoic Acid (4).** To a solution of aldrithiol (4.4 g, 0.02 mol) in ethyl acetate (25 mL) was added dropwise a solution of 3-thiopropionic acid (1.74 mL, 0.02 mol) in ethyl acetate (25 mL). The solution turned immediately to bright yellow after the addition of $BF_3$ ether ethylic complex (4 drops). After the mixture was stirred for 2 h at room temperature, the formation of a yellow precipitate was observed. After 24 h the suspension was filtered (the solid was 2-pyridylmercaptane) and the solvent was removed by evaporation. The oil was dissolved twice in cold ethyl acetate and filtered to give at the end a yellow oil (4.0 g, purity $< 70\%$).

**1-[6,11-Dioxo-7,10-diaza-14,15-dithio-15(2-pyridyl)pentadecanyl]-1,4,7,10-tetraazacyclododecane-4,7,10-triacetic(1,1′-dimethylethyl ester) (5).** *N,N*′-Dicyclohexylcarbodiimide (DCC, 6.2 g, 0.030 mol) was added to a solution of **3** (15.9 g, 0.024 mol) and 3(2-pyridyldithio)propionic acid **4** (5.4 g, 0.025 mol) in dichloromethane (150 mL) under vigorous stirring. After 4 days, the *N,N*′-dicyclohexylurea (DCU) was filtered and the solution was washed with water and brine. The clear solution was evaporated on a rotary evaporator to yield an oil (24.5 g).

**1-[6,11-Dioxo-7,10-diaza-14,15-dithio-15(2-pyridyl)pentadecanyl]-1,4,7,10-tetraazacyclododecane-4,7,10-triacetic Acid (6).** Trifluoroacetic acid (TFA, 46 mL) was added to a solution of **5** (17.4 g, 0.020 mol) in dichloromethane (50 mL). The organic solvent was evaporated on a rotary evaporator. Then a further aliquot of trifluoroacetic acid (46 mL) and triisopropylsilane (500 $\mu$L) was added. After 3 days diethyl ether (300 mL) was added to obtain a white crystalline precipitate that was filtered, washed with diethyl ether (10 mL), and dried. The solid was dissolved in water and purified by liquid chromatography on Amberlite XAD1600 700 mL with a water/methanol gradient (from 0 to 100 in 6 CV). Fractions containing the product were combined and evaporated to a white powder (2.25 g, global yield from **1**, 8.8%). $^1$H NMR (600 MHz, DMSO-$d_6$): $\delta$ 1.24 (m, 2H), 1.53 (m, 4H), 2.10 (t, 2H), 2.54 (o, t, 2H), 2.73 (m, br, 2H), 2.91−3.01 (m, br, TAZA ring), 3.04 (o, t, 2H), 3.13 (m, br, 4H), 3.44 (s, 4H), 3.49 (s, 2H), 7.28 (m, 1H), 7.80 (m, 1H), 7.87 (m, 1H), 8.49 (m, 1H), 8.45 (t, br, 1H, HN), 8.62 (t, br, 1H, NH). $^{13}$C NMR (150 MHz, DMSO-$d_6$, from HMQC/HMBC): $\delta$ 25.6, 26.6, 35.2, 35.7, 36.0, 39.3, 54.4, 56.0, 56.6, 120.1, 122.0, 138.7, 150.6, 160.1, 170.7, 171.8, 172.0, 173.5. MS $[M + H]^+$ calcd for $C_{30}H_{49}N_7O_8S_2$, 699.88; found, 700.2.

**1-[6,11-Dioxo-7,10-diaza-14,15-dithio-15(2-pyridyl)pentadecanyl]-1,4,7,10-tetraazacyclo-dodecane-4,7,10-triacetate ($3^-$) Gadolinate ($3^+$) (1:1) (7).** Gadolinium chloride hexahydrate (149 mg, 0.4 mmol) was added to an aqueous solution of **6** (280 mg, 0.4 mmol). The pH of the solution was slowly brought to neutrality with NaOH, 2 N. Compound **6** (15 mg) was further added in order to obtain an excess of the ligand (about 3%). The solution was filtered on Millipore 0.22 $\mu$m and lyophilized.

**Synthesis of GdL1B. *N*-(Benzyloxycarbonyl)-2-bromoethylamine (13).** A solution of 2-bromoethylamine hydrobromide (71.7 g, 0.35 mol) in water (150 mL) and ethanol (150 mL) was brought with NaOH 10 N at 10 °C to pH 7.1. Benzyl chloroformate (50.0 mL, 0.35 mol) in dimethoxyethane (100 mL) was added to the mixture dropwise over 2 h at $< 20$ °C, and the pH was maintained at 7. After 16 h at room temperature the organic phase was removed by evaporation and the product was extracted with dichloromethane ($3 \times 50$ mL). The organic layer was washed with water, HCl 0.1 N, water, brine, dried, and evaporated to give a white solid (79.8 g). $^1$H NMR (300 MHz, $CD_3OD$): $\delta$ 3.30 (t, 2H), 3.61 (t, 2H), 5.12 (s, 2H), 7.38 (m, 5H). $^{13}$C NMR(300 MHz, $CD_3OD$): $\delta$ 20.8, 42.7, 66.5, 127.9, 128.2, 128.6, 137.3, 157.8.

**1-[*N*-(benzyloxycarbonyl)-2-aminoethyl]-1,4,7,10-tetraazacyclododecane-4,7,10-triacetic(1,1-dimethylethyl ester) (14).** DO3A-tris-*tert*-butyl ester (37.1 g, 0.072 mol, free base) was dissolved in acetonitrile (150 mL), and $K_2CO_3$ (11.9 g, 0.086 mol) was added. The mixture was kept under stirring at room temperature while a solution of **13** (20.4 g, 0.079 mol) in acetonitrile (150 mL) was added dropwise over a period of 1 h. The reaction mixture was kept under stirring for 4 days at 50 °C. After filtration the solvent was removed by evaporation under reduced pressure and the residue treated with diethyl ether (100 mL) to give a white solid corresponding to unreacted parent **16**. After filtration the solution was evaporated in vacuo and the residue purified by flash chromatography on silica with a dichloromethane/methanol gradient. Fractions containing the product were combined and evaporated to give a yellow oil (34 g). $^1$H NMR (300 MHz, $CD_3OD$): $\delta$ 1.48 (s, 27H), 1.70−3.18 (b m, 26H), 5.18 (s, 2H), 7.38 (m, 5H). MS $[M + H^+]$ calcd, 691.9; found, 692.83.

**1-(2-Aminoethyl)-1,4,7,10-tetraazacyclododecane-4,7,10-triacetic(1,1-dimethylethyl ester) (15).** Compound **14** (34.0 g, 0.049 mol) was dissolved in methanol (200 mL), and 10% Pd/C (2.0 g) was added. Then the reaction was carried out under hydrogen atmospheric pressure at room temperature for 6 h. The mixture was then filtered and the solvent evaporated (28.6 g). $^1$H NMR (300 MHz, $CD_3OD$): $\delta$ 1.45 (s, 27H), 1.85−3.24 (b m, 26H). MS $[M + H^+]$ calcd, 557.77; found, 558.65.

**1-[*N*-[3(2-Pyridyldithio)propanoyl]2-aminoethyl]-1,4,7,10-tetraazacyclododecane-4,7,10-triacetic(1,1-dimethylethyl ester) (17).** A solution of **4** (4.0 g, 0.015 mol, purity of ~70%) in ethyl acetate (20 mL) was added to a solution of **15** (5.0 g, 0.009 mol) in ethyl acetate (20 mL). Then triethylamine (1.4 mL, 0.01 mol) and dicyclohexylcarbodiimide (3.7 g, 0.018 mol) were added and the mixture was left stirring at room temperature for 4 days. After dicyclohexylurea was filtered away, the organic phase was washed with water, $NaHCO_3$ 1%, and brine. The solvent was evaporated to give a yellow oil (11 g, purity of $< 60\%$). $^1$H NMR (300 MHz, $CD_3OD$): $\delta$ 1.49 (s, 27H), 2.58 (t, 2H), 3.17 (t, 2H), 7.24 (m, 1H), 7.73 (m, 2H), 8.42 (m, 1H). MS $[M + H^+]$ calcd, 755.04; found, 755.66.

**1-[*N*-[3(2-Pyridyldithio)propanoyl]2-aminoethyl]-1,4,7,10-tetraazacyclododecane-4,7,10-triacetic Acid (18).** The compound was obtained by a route similar to that of **11** and purified by liquid chromatography on Amberchrom CG161 resin with a water−methanol gradient. Fractions containing the product were combined and evaporated to give a white solid (400 mg). $^1$H NMR (300 MHz, $D_2O$): $\delta$ 2.46 (t, 2H), 2.87 (t, 2H), 2.91−3.75 (b m, 26H), 7.15 (t, 1H), 7.71 (m, 2H), 8.23 (t, 1H). $^{13}$C NMR (300 MHz, $D_2O$): $\delta$ 33.9, 34.8, 36.3, 48.5, 48.8, 50.7, 51.2, 51.6, 54.0, 56.5, 121.9, 122.4, 140.0, 149.1, 158.9, 171.0, 174.8. MS $[M + H^+]$ calcd, 557.77; found, 558.65.

**1-[*N*-[3(2-Pyridyldithio)propanoyl]2-aminoethyl]-1,4,7,10-tetraazacyclododecane-4,7,10-triacetate ($3^-$) Gadolinate ($3^+$) (1:1) (19).** The complexation was performed with $GdCl_3$ in aqueous solution at pH 7 by the method of the addition of the ligand. An equimolar amount of $GdCl_3$ (127 mg, 0.34 mmol) solution in water was added to the aqueous solution of ligand (200 mg, 0.34 mmol), maintaining the pH at 7 with NaOH 0.1 N. The mixture was allowed to stir at room temperature until the pH remained constant at 7. The solution was then lyophilized to give a white solid (350 mg). The amount of residual free $Gd^{3+}$ ion was assessed by the orange xylenol spectrophotometric assay,[27] and a suitable amount of ligand was added to have a slight excess of the ligand (about 3%) and to avoid the presence of free Gd(III) ions.

**Synthesis of GdL2A. *N,N*′-Bis[2-[bis[2-(1,1-dimethylethoxy)-2-oxoethyl]amino]ethyl]-L-*N*-[3-[(2-pyridyl)dithio]propionyl]lysine(1,1-dimethylethyl ester) (21).** A solution of *N,N*′-bis[2-[bis-[2-(1,1-dimethylethoxy)-2-oxoethyl]-amino]ethyl]-L-lysine(1,1-dimethylethyl ester) **20** (9.7 g, 0.013 mol) in dichloromethane (30 mL) was added to a solution of **4** (3.64, 0.013 mol) in dichloromethane (20 mL). Then dicyclohexylcarbodiimide

(3.20 g, 0.0156 mol) was added and the mixture was left under stirring for 32 h at room temperature. After dicyclohexylurea was filtered away, the organic phase was washed with $NaCO_3$ 5%, water, brine and dried with $Na_2SO_4$. After filtration, the solution was concentrated to give an oil (12.8 g) that was purified by flash chromatography on silica with a hexane/ethyl acetate gradient. Fractions containing the product were combined and evaporated to give a yellow oil (1.90 g). MS $[M + H^+]$ calcd, 942.28; found, 942.95.

***N,N′*-Bis[2-[bis[carboxymethyl]amino]ethyl]-L-*N*-[3-[(2-pyridyl)-dithio]propionyl]lysine (22).** Neat trifluoroacetic acid (0.71 mL, 0.0097 mol) was slowly added to a solution of **21** (1.40 g, 0.001 319 mol) in dichloromethane (5 mL) and the mixture stirred at room temperature for 1 h. Dichloromethane was evaporated and the residue treated with trifluoroacetic acid (5.0 mL) and triisopropylsilane (0.10 mL). The solution was stirred for 24 h. Then diethyl ether was slowly added (20 mL) to give a precipitate which was filtered, washed with diethyl ether, and dried (0.82 g). $^1$H NMR (300 MHz, $CD_3OD$): $\delta$ 1.09 (t, 2 H), 1.42 (m, 3 H), 1.55 (m, 2 H), 1.76 (m, 2 H), 2.60 (m, 2 H), 3.09 (m, 10 H), 3.46 (m, 8 H), 7.70 (t, 1 H), 8.13 (d,1 H), 8.30 (t,1 H), 8.56 (d,1 H). $^{13}$C NMR (600 MHz, $D_2O$): $\delta$ 14.4, 23.7, 28.0, 34.8, 39.4, 46.4, 53.2, 56.4, 63.6, 66.4, 115.7, 124.2, 125.6, 143.4, 145.5, 163.2, 170. MS $[M + H^+]$ calcd, 661.64; found, 662.34.

***N,N′*-Bis[2-[bis[carboxymethyl]amino]ethyl]-L-*N′*-[3-[(2-pyridyl)dithio]propionyl]lysinate ($5^-$) Gadolinate ($3^+$) (1:1) Sodium Salt (1:2) (23).** An equimolar amount of aqueous $GdCl_3$ (438 mg, 0.41 mmol) was added to the aqueous solution of ligand (107 mg, 0.41 mmol), maintaining the pH at 7 with NaOH 0.1 N. The mixture was kept under stirring at room temperature until the pH remained constant at 7. The solution was then lyophilized to give a white solid (350 mg). The amount of residual free $Gd^{3+}$ ion was assessed by the orange xylenol spectrophotometric method, and a suitable amount of ligand was added to have an excess of the ligand of 2%. MS $[M + H^+]$ calcd, 814.96; found, 815.45.

**Synthesis of GdL2B. L-*S*-(2-Pyridylthio)cysteine $BF_3$ Salt (8).** L-Cysteine (2.4 g, 0.02 mol) was added into a solution of aldrithiol (4.4 g, 0.02 mol) in ethyl acetate (50 mL). Then $BF_3$ ether ethylic complex (1.5 mL, 0.02 mol) was added dropwise to the suspension, which immediately became bright yellow. After 4 days at room temperature, the suspension was filtered and the yellow solid washed several times with cold ethyl acetate, filtered again, and dried (3.8 g).

***N,N′*-Bis[2-[bis[2-(1,1-dimethylethoxy)-2-oxoethyl]amino]ethyl]-L-*S*-(2-pyridylthio)cysteine (10).** A solution of **9** (9.9 g, 0.0268 mol) in acetonitrile (30 mL) was added to a suspension of **8** (3.8 g, 0.016 mol) and DIPEA (1.05 mL, 0.019 mol) in acetonitrile (50 mL). After 24 h at room temperature the suspension was filtered and the solution recovered and concentrated to give an oil, which was washed with diethyl ether and then hexane. The product was insoluble in hexane, and it was purified by flash chromatography on silica by a diethyl ether/methanol gradient. The fractions containing the product were combined and evaporated to give a yellow oil (2.9 g). $^1$H NMR (300 MHz, $CD_3OD$): $\delta$ 1.51 (s, 27H), 2.45 (m, 1H), 2.56 (m, 1H), 2.98 (t, 4H), 3.15 (t, 4H), 4.05 (m, 1H), 7.32 (m, 1H), 7.71 (m, 2H), 7.96 (m, 1H), 8.47 (m, 1H). MS $[M + H^+]$ calcd, 773.01; found, 774.26.

***N,N′*-Bis[2-[bis[carboxymethylen]amino]ethyl]-L-*S*-(2-pyridylthio)cysteine (11).** Neat trifluoroacetic acid (1.9 mL, 0.025 mol) was slowly added to a solution of **10** (1.3 g, 0.0017 mol) in dichloromethane (5 mL) and the mixture stirred at room temperature for 1 h. Dichloromethane was evaporated and the residue treated with trifluoroacetic acid (8.0 mL, 0.10 mol) and triisopropylsilane (0.2 mL). The solution was stirred for 24 h. Then diethyl ether was slowly added (20 mL) to give a slightly yellow solid, which was filtered, washed with diethyl ether, and dried (0.82 g).

**[*N,N′*-Bis[2-[bis[carboxymethylen]amino]ethyl]-L-*S*-(2-pyridylthio)cysteinate ($5^-$)] Gadolinate ($3^+$) (1:1) Sodium Salt (1:2) (12).** Since ligand **11** (290 mg, 0.2 mmol) was not stable in water, the complexation was performed very quickly by adding an equimolar amount of $GdCl_3$ (83 mg, 0.2 mmol) in aqueous solution at pH 7. The solution was then quickly lyophilized to give a pale-yellow solid (350 mg). The concentration of the Gd was determined by $^1$H NMR $T_1$ measurement of the mineralized complex (in HCl 37% at 120 °C for 16 h), while the concentration of the ligand was determined by UV−vis spectrophotometry.[19]

**Cell Culture.** The culture media DMEM F-12, DEME, RPMI 1640, and fetal bovine serum (FBS) were purchased from Cambrex, East Rutherford, NJ. All other supplements/chemicals were from Sigma Chemical Co., St Louis, MO. Human myeloid leukemia (K562) cells were cultured in RPMI 1640 supplemented with 10% fetal bovine serum (FBS), 100 U/mL penicillin, and 100 U/mL streptomycin. Cell were cultured in a humidified 95:5 v/v air/$CO_2$ atmosphere and serially passaged in 75 cm$^2$ tissue culture flasks. For uptake experiments, 3 millions cells were recovered and suspended in 2 mL of a incubation medium in 6 cm Petri dishes. Rat glioma (C6) and murine melanoma (B16) cells were cultured in DMEM F-12 and DEME media, supplemented as described above with the exception of FBS, which was 5%. C6 and B16 cells were detached with a 0.25% trypsin−EDTA solution when confluence was about 80%. For uptake experiments, C6 and B16 cells were seeded in 6 cm Petri dishes at a density of $4 \times 10^4$ cell/cm$^2$. Twenty-four hours after seeding cells were ready for the uptake experiments.

The trypan blue exclusion test was used to assess cell viability. An amount of 10 $\mu$L of each cell suspension was added to 10 $\mu$L of 0.4% trypan blue solutions in PBS. The suspended cells, once introduced in a counting chamber, appear round and bright when viable and colored in deep blue when damaged.

The growth curve of K562 cells was obtained by harvesting cells from a 75 cm$^2$ flask every 24 h for up to 13 days. After being harvested, cells were stained with trypan blue and live cells counted with a counting chamber. The RPMI 1640 culture medium was renewed every 24 h.

**Spectrophotometric Assay for EPTs.** The amount of cell-surface protein thiols was determined using the DTNB test.[22] Cells were suspended in 1 mL of HEPES buffer, and DTNB was added to a final concentration of 200 $\mu$M. After 30 min of incubation at room temperature, cells were pelleted and the 2-nitro-5-thiobenzoic acid content of the supernatant was evaluated by measuring the absorbance at 412 nm ($\varepsilon$ = 14 150 M$^{-1}$ cm$^{-1}$).

**Cell Labeling.** The typical labeling procedure consisted of incubating 3−5 million cells for 4 h at 37 °C in a minimum medium (Earl's balanced salt solution, EBSS, in which the phosphate has been replaced by 1.2 mM HEPES sodium salt) containing the Gd-based labeling agent in a typical concentration range of 0.5−4.0 mM. In experiments with lactate, lactate was added up to 15 mM just before addition of the labeling agent. In the experiments carried out at 37 °C, cells were incubated for 4 h in $CO_2$−air (5:95) atmosphere, while for experiments at 4 °C cells were incubated for a maximum of 1 h in a sterile environment. After incubation the cells were washed three times with 5 mL of HEPES buffer. For C6 and B16 lines, cells were recovered mechanically by harvesting them in 200 mL of HEPES with a scraper. After recovering from the labeling medium, cells were washed and suspended in 200 mL of HEPES and then sonicated for 10 s for a complete lysis. HCl 37% was added at the same volume, and the mixture was left at 120 °C overnight. Upon this treatment all Gd(III) was released as the free aquo ion. By measurement of the water proton relaxation rate of these solutions, it is possible to determine its concentration.[12,26] Relaxation rate measurements were performed at 20 MHz and 25 °C on a Spinmaster spectrometer (Stelar, Mede, Italy) by using a conventional inversion recovery pulse sequence. The obtained $R_{1obs}$ data are related to the concentration of the paramagnetic species according to the formula

$$R_{1obs} = R_{1W} + [Gd(III)]r_{1p}^{Gd(III)}$$

where $R_{1W}$ is the relaxation rate of pure water (0.38 $s^{-1}$) and $r_{1p}^{Gd(III)}$ the millimolar relaxivity of the Gd(III) aquo ion (13.5 $mM^{-1} s^{-1}$ in 6 M HCl, 25 °C). This method was calibrated using standard ICP solutions, and the accuracy was determined to be within 1%. The moles of Gd(III) obtained in this way were normalized against the weight (in milligrams) of cellular proteins. The protein concentration of each sample was determined from cell lysates by the Bradford method[41] using bovine serum albumin as the standard.

**$^1$H NMR and $^{17}$O NMR Relaxation Rate Measurements.** The longitudinal water proton relaxation rate was measured by using a Stelar Spinmaster (Stelar, Mede, Pavia, Italy) spectrometer operating at 20 MHz by means of the standard inversion recovery sequence. The temperature was controlled with a Stelar VTC-91 air-flow heater equipped with a copper constantan thermocouple (uncertainty of 0.1 °C). The proton $1/T_1$ NMRD profiles were measured over a continuum of magnetic field strength from 0.000 24 to 0.47 T (corresponding to 0.01−20 MHz proton Larmor frequency) on a Stelar field-cycling relaxometer. The relaxometer works under complete computer control with an absolute uncertainty in $1/T_1$ of ±1%. Data points from 0.47 T (20 MHz) to 1.7 T (70 MHz) were collected on a Stelar Spinmaster spectrometer working at variable field. The concentrations of Gd complex solutions, for the relaxometric characterization, were determined by the relaxometric procedure as described above.

For variable-temperature $^{17}$O NMR measurements, aqueous solutions containing 2.6% $^{17}$O isotope (Yeda, Israel) were used. Variable-temperature $^{17}$O NMR measurements were recorded at 600 MHz on a Bruker spectrometer, equipped with a 5 mm probe, using a $D_2O$ external lock. Experimental settings were as follows: spectral width of 9000 Hz, 90° pulse for 14 μs, acquisition time of 10 ms, 1024 scans, and no sample spinning. The observed transverse relaxation rates $R^0_{2p}$obs were calculated from the signal width at half-height ($\Delta\nu_{1/2}$): $R^0_{2p}obs = \pi\Delta\nu_{1/2}$

**MRI Experiments.** To acquire "in vitro" MR images, cells were transferred into glass capillaries that were centrifuged at 1500*g* for 5 min and placed in an agar phantom. MR images were acquired on a Bruker Avance 300 spectrometer operating at 7 T equipped with a microimaging probe (birdcage resonator with 10 mm inner diameter). Images were acquired with a standard $T_1$-weighted multislice multiecho sequence (TR/TE/NEX = 250/3.3/6, FOV 1.15 cm, 1 slice 1 mm). Measurement of $T_1$ was performed by using a saturation recovery spin echo sequence (TE = 2.6 ms, 16 variable TR ranging from 40 to 1000 ms, NEX = 1, FOV = 1.1 cm, 1 slice 1 mm).

**Acknowledgment.** Economic and scientific support from MIUR (PRIN 2005039914 projects), EC-FP6 projects DiMI (Grant LSHB-CT-2005-512146), MEDITRANS (Targeted Delivery of Nanomedicine: Grant NMP4-CT-2006-026668), EU-FP7-HEALTH-2007-1.2-4 ENCITE (European Network for Cell Imaging and Tracking Expertise), and Regione Piemonte (POR-FESR Asse I I.1.1 "PIIMDMT"; Ricerca Sanitaria Finalizzata, bando 2008bis; Bando Converging Technologies BIO-THER) is gratefully acknowledged.

**Supporting Information Available:** Representative control data for GdDO3A. This material is available free of charge via the Internet at http://pubs.acs.org.

## References

(1) Krestin, G. P.; Bernsen, M. R. Molecular imaging in radiology: the latest fad or the new frontier? *Eur. Radiol.* **2006**, *16*, 2383–2385.
(2) Weissleder, R.; Mahmood, U. Molecular imaging. *Radiology* **2001**, *219*, 316–333.
(3) Modo, M. M. J. J., Bulte, J .W. M., Eds. *Molecular and Cellular MR-Imaging*; CRC Press: Boca Raton, FL, 2007.
(4) Pathak, A. P.; Gimi, B.; Glunde, K.; Ackerstaff, E.; Artemov, D.; Bhujwalla, Z. M. Molecular and functional imaging of cancer: advances in MRI and MRS. *Methods Enzymol.* **2004**, *386*, 3–60.
(5) Aime, S.; Cabella, C.; Colombatto, S.; Geninatti-Crich, S.; Gianolio, E.; Maggioni, F. Insights into the use of paramagnetic Gd(III) complexes in MR-molecular imaging investigations. *J. Magn. Reson. Imaging* **2002**, *16*, 394–406.
(6) Muller, R. N.; Roch, A.; Colet, J.-M.; Ouaksim, A.; Gillis, P. Particulate Magnetic Constrast Agents. In *The Chemistry of Contrast Agents in Medical Magnetic Resonance Imaging*; Merbach, A. E., Tóth, E., Eds.; John Wiley & Sons: Chichester, U.K., 2001; pp 417−435.
(7) Bulte, J. W. M.; Kraitchman, D. L. Iron oxide MR contrast agents for molecular and cellular imaging. *NMR Biomed.* **2004**, *17*, 484–499.
(8) Lewin, M.; Carlesso, N.; Tung, C. H.; Tang, X. W.; Cory, D.; Scadden, D. T.; Weissleder, R. Tat peptide-derivatized magnetic nanoparticles allow in vivo tracking and recovery of progenitor cells. *Nat. Biotechnol.* **2000**, *18*, 410–414.
(9) Caravan, P.; Ellison, J. J.; McMurry, T. J.; Lauffer, R. B. Gadolinium(III) chelates as MRI contrast agents: structure, dynamics, and applications. *Chem. Rev.* **1999**, *99*, 2293–2353.
(10) Wiener, E. C.; Konda, S.; Shadron, A.; Brechbiel, M.; Gansow, O. Targeting dendrimer-chelates to tumors and tumor cells expressing the high-affinity folate receptor. *Invest. Radiol.* **1997**, *32*, 748–754.
(11) Geninatti Crich, S.; Cabella, C.; Barge, A.; Belfiore, S.; Ghirelli, C.; Lattuada, L.; Lanzardo, S.; Mortillaro, A.; Tei, L.; Visigalli, M.; Forni, G.; Aime, S. In vitro and in vivo magnetic resonance detection of tumor cells by targeting glutamine transporters with Gd-based probes. *J. Med. Chem.* **2006**, *49*, 4926–4936.
(12) Geninatti Crich, S.; Biancone, L.; Cantaluppi, V.; Duò, D.; Esposito, G.; Russo, S.; Camussi, G.; Aime, S. Improved route for the visualization of stem cells labeled with a Gd-/Eu-chelate as dual (MRI and fluorescence) agent. *Magn. Reson. Med.* **2004**, *51*, 938–944.
(13) Biancone, L.; Geninatti Crich, S.; Cantaluppi, V.; Mauriello Romanazzi, G.; Russo, S.; Scalabrino, E.; Esposito, G.; Figliolini, F.; Beltramo, S.; Cavallo Perin, P.; Segoloni, G. P.; Aime, S.; Camussi, G. Magnetic resonance imaging of gadolinium-labeled pancreatic islets for experimental transplantation. *NMR Biomed.* **2007**, *20*, 40–48.
(14) Terreno, E.; Geninatti Crich, S.; Belfiore, S.; Biancone, L.; Cabella, C.; Esposito, G.; Manazza, S. D.; Aime, S. Effect of the intracellular localization of a Gd-based imaging probe on the relaxation enhancement of water protons. *Magn. Reson. Med.* **2006**, *55*, 491–497.
(15) Strijkers, G. J.; Hak, S.; Kok, M. B.; Springer, C. S.; Nicolay, K. Three-compartment $T_1$ relaxation model for intracellular paramagnetic contrast agents. *Magn. Reson. Med.* **2009**, *61*, 1049–1058.
(16) Endres, P. J.; MacRenaris, K. W.; Vogt, S.; Meade, T. J. Cell-permeable MR contrast agents with increased intracellular retention. *Bioconjugate Chem.* **2008**, *19*, 2049–2059.
(17) Gianolio, E.; Giovenzana, G. B.; Ciampa, A.; Lanzardo, S.; Imperio, D.; Aime, S. A novel method of cellular labeling: anchoring MR-imaging reporter particles on the outer cell surface. *ChemMedChem* **2008**, *3*, 60–62.
(18) Digilio, G.; Catanzaro, V.; Fedeli, F.; Gianolio, E.; Menchise, V.; Napolitano, R.; Gringeri, C.; Aime, S. Targeting exofacial protein thiols with Gd-III complexes. An efficient procedure for MRI cell labeling. *Chem. Commun.* **2009**, 893–895.
(19) Carrera, C.; Digilio, G.; Baroni, S.; Burgio, D.; Consol, S.; Fedeli, F.; Longo, D.; Mortillaro, A.; Aime, S. Synthesis and characterization of a Gd(III) based contrast agent responsive to thiol containing compounds. *Dalton Trans.* **2007**, 4980–4987.
(20) Laragione, T.; Gianazza, E.; Tonelli, R.; Bigini, P.; Mennini, T.; Casoni, F.; Massignan, T.; Bonetto, V.; Ghezzi, P. Regulation of redox-sensitive exofacial protein thiols in CHO cells. *Biol. Chem.* **2006**, *387*, 1371–1376.
(21) Sahaf, B.; Heydari, K.; Herzenberg, L. A.; Herzenberg, L. A. Lymphocyte surface thiol levels. *Proc. Natl. Acad. Sci. U.S.A.* **2003**, *100*, 4001–4005.
(22) Jiang, X.-M.; Fitzgerald, M.; Grant, C. M.; Hogg, P. J. Redox control of exofacial protein thiols/disulfides by protein disulfide isomerase. *J. Biol. Chem.* **1999**, *274*, 2416–2423.
(23) Laragione, T.; Sonetto, V.; Casoni, F.; Massignan, T.; Bianchi, G.; Gianazza, E.; Ghezzi, P. Redox regulation of surface protein thiols: identification of integrin α-4 as a molecular target by using redox proteomics. *Proc. Natl. Acad. Sci. U.S.A.* **2003**, *100*, 14737–14741.
(24) Dominici, S.; Valentini, M.; Maellaro, E.; Del Bello, B.; Paolicchi, A.; Lorenzini, E.; Tongiani, R.; Comporti, M.; Pompella, A. Redox modulation of cell surface protein thiols in U937 lymphoma cells: the role of the γ-glutamyl transpeptidase dependent $H_2O_2$ production and S-thiolation. *Free Radical Biol. Med.* **1999**, *27*, 623–635.

(25) Anelli, P. S.; Fedeli, F.; Gazzotti, O.; Lattuada, L.; Lux, G.; Rebasti, F. L-Glutamic acid and L-lysine as useful building blocks for the preparation of bifunctional DTPA-like ligands. *Bioconjugate Chem.* **1999**, *10*, 137–140.
(26) Cabella, C.; Geninatti Crich, S.; Corpillo, D.; Barge, A.; Ghirelli, C.; Bruno, E.; Lorusso, V.; Uggeri, F.; Aime, S. Cellular labeling with Gd(III) chelates: only high thermodynamic stabilities prevent the cells acting as sponges of $Gd^{3+}$ ions. *Contrast Media Mol. Imaging* **2006**, *1*, 23–29.
(27) Geninatti Crich, S.; Lanzardo, S.; Barge, A.; Esposito, G.; Tei, L.; Forni, G.; Aime, S. Visualization through magnetic resonance imaging of DNA internalized following "in vivo" electroporation. *Mol. Imaging* **2005**, *4*, 7–17.
(28) Banci, L.; Bertini, I.; Luchinat, C. *Nuclear and Electronic Relaxation*; VCH: Weinheim, Germany, 1991.
(29) Aime, S.; Geninatti Crich, S.; Gianolio, E.; Giovenzana, G. B.; Tei, L.; Terreno, E. High sensitivity lanthanide(III) based probes for MR-medical imaging. *Coord. Chem. Rev.* **2006**, *250*, 1562–1579.
(30) Aime, S.; Gianolio, E.; Terreno, E.; Giovenzana, G. B.; Pagliarin, R.; Sisti, M.; Palmisano, G.; Botta, M.; Lowe, M. P.; Parker, D. Ternary Gd(III)L-HSA adducts: evidence for the replacement of inner-sphere water molecules by coordinating groups of the protein. Implications for the design of contrast agents for MRI. *JBIC, J. Biol. Inorg. Chem.* **2000**, *5*, 488–497.
(31) Aime, S.; Botta, M.; Geninatti Crich, S.; Giovenzana, G.; Pagliarin, R.; Sisti, M.; Terreno, E. NMR relaxometric studies of Gd(III) complexes with heptadentate macrocyclic ligands. *Magn. Reson. Chem.* **1998**, *36*, S200–S208.
(32) Powell, D. H.; Ni Dhubhghaill, O. M.; Pubanz, D.; Helm, L.; Lebedev, Y. S.; Schlaepfer, W.; Merbach, A. E. Structural and dynamic parameters obtained from O-17 NMR, EPR, and NMRD studies of monomeric and dimeric $Gd^{3+}$ complexes of interest in magnetic resonance imaging: an integrated and theoretically self consistent approach. *J. Am. Chem. Soc.* **1996**, *118*, 9333–9346.
(33) Aime, S.; Botta, M.; Fasano, M.; Terreno, E. Prototropic and water-exchange processes in aqueous solutions of Gd(III) chelates. *Acc. Chem. Res.* **1999**, *32*, 941–949.
(34) Aime, S.; Botta, M.; Fasano, M.; Terreno, E. Protein-Bound Metal Chelates. In *The Chemistry of Contrast Agents in Medical Magnetic Resonance Imaging*; Merbach, A. E., Tóth, E., Eds.; John Wiley & Sons: Chichester, U.K., 2001; pp 193−241.
(35) Aime, S.; Botta, M.; Bruce, J. L.; Mainero, V.; Parker, D.; Terreno, E. Modulation of the water exchange rates in Gd-DO3A complex by formation of ternary complexes with carboxylate ligands. *Chem Commun.* **2001**, 115–116.
(36) Botta, M.; Aime, S.; Barge, A.; Bobba, G.; Dickins, R. S.; Parker, D.; Terreno, E. Ternary complexes between cationic Gd(III) chelates and anionic metabolites in acqueous solution: an NMR relaxometric study. *Chem.—Eur. J.* **2003**, *9*, 2102–2109.
(37) Terreno, E.; Botta, M.; Boniforte, P.; Bracco, C.; Milone, L.; Mondino, B.; Uggeri, F.; Aime, S. A multinuclear NMR relaxometry study of ternary adducts formed between heptadentate Gd(III) chelates and L-lactate. *Chem.—Eur. J.* **2005**, *11*, 5531–5537.
(38) Hogg, P. J. Disulfide bonds as switches for protein function. *Trends Biochem. Sci.* **2003**, *28*, 211–214.
(39) Go, Y.-M.; Jones, D. P. Intracellular proatherogenic events and cell adhesion modulated by extracellular thiol/disulfide redox state. *Circulation* **2005**, *111*, 2973–2980.
(40) Ghezzi, P. Oxidoreduction of protein thiols in redox regulation. *Biochem. Soc. Trans.* **2005**, *33*, 1378–1381.
(41) Bradford, M. M. A rapid and sensitive method for the quantitation of microgram quantities of protein utilizing the principle of protein−dye binding. *Anal. Biochem.* **1976**, *72*, 248–254.